Separation Science and Technology
Publication details, including instructions for authors and subscription information:
http://www.informaworld.com/smpp/title~content=t713708471

Particle Flocculation and Filtration by High-Gradient Magnetic Fields

C. Tsouris[a]; S. Yiacoumi[b]
[a] Oak Ridge National Laboratory, Oak Ridge, Tennessee [b] Georgia Institute of Technology School of Civil and Environmental Engineering, Atlanta, Georgia

To cite this Article Tsouris, C. and Yiacoumi, S.(1997) 'Particle Flocculation and Filtration by High-Gradient Magnetic Fields', Separation Science and Technology, 32: 1, 599 — 616
To link to this Article: DOI: 10.1080/01496399708003218
URL: http://dx.doi.org/10.1080/01496399708003218

SEPARATION SCIENCE AND TECHNOLOGY, 32(1-4), pp. 599-616, 1997

PARTICLE FLOCCULATION AND FILTRATION BY HIGH-GRADIENT MAGNETIC FIELDS*

C. Tsouris
Oak Ridge National Laboratory
P.O. Box 2008
Oak Ridge, Tennessee 37831-6226

S. Yiacoumi
Georgia Institute of Technology
School of Civil and Environmental Engineering
Atlanta, Georgia 30332-0512

ABSTRACT

Flocculation and filtration of micrometer-sized particles in a high-gradient magnetic field (HGMF) were investigated. Experiments were conducted using a cryogenic magnet of 6 Tesla maximum strength. Hematite particles were used for flocculation and filtration experiments. A new approach of using magnetic fields to enhance separation of weakly magnetic particles was also investigated. This approach is based on magnetic seeding which involves flocculation of existing non-magnetic particles with injected paramagnetic particles. A particle-flocculation model was developed based on trajectory analysis. External forces due to gravity and magnetism, and interparticle forces such as electrostatic, hydrodynamic, magnetic dipole, and van der Waals forces, were taken into consideration in these models.

* This research was supported by the Division of Chemical Sciences, Office of Basic Energy Sciences, the AR&TD program of Fossil Energy, and the Efficient Separations and Processing Crosscutting Program, Office of Environmental Management, U.S. Department of Energy, under contract DE-AC05-96OR22464 with Lockheed Martin Energy Research Corp. Accordingly, the U.S. Government retains a nonexclusive, royalty-free license to publish or reproduce the published form of this contribution, or allow others to do so, for U.S. Government purposes.

INTRODUCTION

In terms of their magnetic properties, materials may be divided in various groups: ferromagnetic materials have magnetic susceptibility (i.e., the ratio of magnetization to the magnetic field strength) of order 1, paramagnetic materials have positive magnetic susceptibility in the range of 10^{-3}-10^{-5}, and diamagnetic materials have negative magnetic susceptibility in the proximity of -10^{-5}. Also, some materials having magnetic susceptibility between ferromagnetic and paramagnetic are called super-paramagnetic. Based on differences of the magnetic susceptibility of materials, magnetic separation has been introduced as a recovery and pollution control process for many environmental and industrial problems, including treatment of the effluents from steel mills (1), desulfurization of coal (2), separation of mining ores and wastes (3), clay processing (4), filtration of the coolant water of nuclear reactors (5), separation of yeast in bioprocessing (6), purification of drinking water (7), and treatment of wastewater (8). The idea of using strong and high-gradient magnetic fields (HGMFs) to separate weakly magnetic particles has been recently introduced (1). Phenomena of interest in magnetic separations are: (a) particle flocculation due to induced dipole-dipole interactions and (b) particle filtration by HGMFs.

In this study, experiments were conducted to investigate the efficiency of high-gradient magnetic filtration (HGMF) of colloidal hematite (paramagnetic) particles. This process can be analyzed by studying particle-collector and particle-particle interactions. The development of a modeling approach to describe particle-particle interactions and understand the mechanism of particle flocculation in homogeneous and high-gradient magnetic fields is discussed. Studies of particle-particle interactions have led to the introduction of magnetic-seeding flocculation as a process to separate nonmagnetic particles by flocculation with small amounts of injected magnetic particles. The flocs consisting of low and high magnetic-susceptibility particles can respond and thus be separated in a high-gradient magnetic filter. Preliminary results of magnetic-seeding flocculation are presented here.

EXPERIMENTAL

The experimental system for HGMF experiments is shown in Figure 1 (9). A split-coil cryogenic magnet (model 110, American Magnetics Inc.), with "warm-

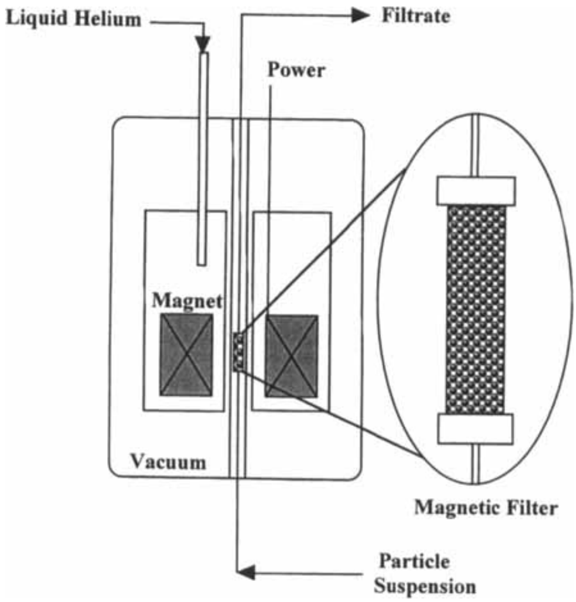

FIGURE 1. Experimental system for HGMF.

bore" optical access in the vertical direction and every 90° in the horizontal plane, provides a uniform magnetic field of 6 Tesla (T=V s m^{-2}) maximum strength at the center where the magnetic filter is placed. The coil is made of niobium-titanium material that has superconducting properties at liquid helium temperature (4.2 K). A magnetic filter of 40-mm length, 6-mm outside diameter, 4-mm inside diameter, and 1.5-mL free space, packed with ferromagnetic spheres of 1.6-mm diameter has been constructed and tested in a high-gradient magnetic field with hematite particles (detail in Figure 1). The hematite particles used in this study (Figure 2) have been produced in our laboratory by the sol-gel method of Sugimoto et al. (10). A high-gradient magnetic filtration experiment was operated at a flow rate of 3.9 mL/min for several hundred filter-bed volumes with a feed concentration of 200 ppm of submicron hematite particles. Data from this experiment, comparing hematite particle concentration in the effluent from the magnetic filter (filtrate) with and without a 1-Tesla magnetic field applied, are presented in Figure 3. No particle breakthrough was observed after 3 hours of operation with the magnetic

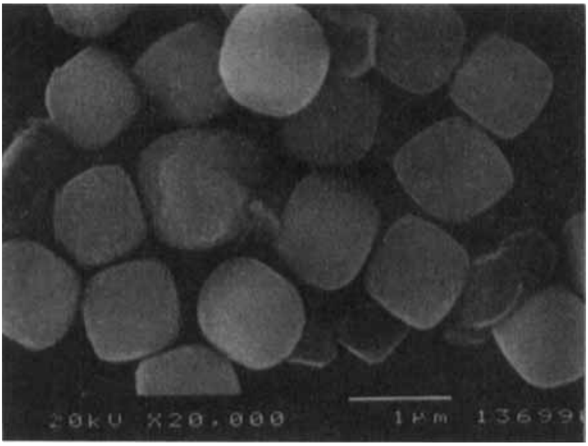

FIGURE 2. Hematite particles produced by the sol-gel method of Sugimoto et al. (10) for HGMF experiments.

field applied, indicating that a high separation efficiency of the particles and flocs of interest may be achieved.

The data of Figure 3 show that HGMF is an effective separation method for weakly magnetic particles. Fundamental particle phenomena occurring in the magnetic bed during the HGMF experiment are particle-particle and particle-collector collisions. A mathematical description of these phenomena is expected to elucidate the mechanisms of flocculation and filtration by HGMF and eventually yield a predictive tool that can be used for the design of efficient magnetic filters.

In another experiment, flocculation of simulated-waste particle suspensions containing strontium was investigated by turbidity measurements. The objective of this experiment was to qualitatively study the effect on magnetic flocculation by seeding the original particle suspension with super-paramagnetic particles. The seeding particles were spherical, micron-sized polystyrene particles (Bangs Laboratories, Inc.) containing 23.8% magnetite (Fe_3O_4) and suspended in water in a concentration of 323 mg/L. A volume ratio of 1:1 was

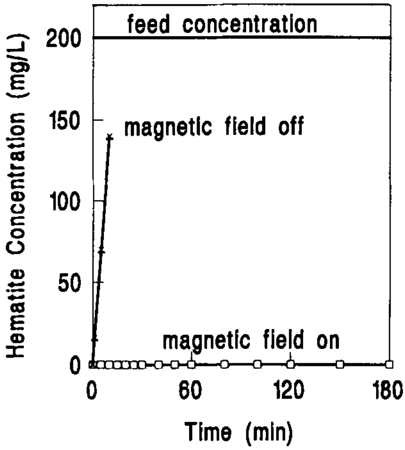

FIGURE 3. HGMF of hematite particles under 1-Tesla magnetic field; suspension flow-rate: 3.9 mL/min.

used from each particle suspension. A comparison of light-intensity measurements from magnetically seeded and non-seeded particle suspensions with and without the magnetic field is shown in Table 1. The relative turbidity is defined as $[V_f-V_t] / [V_f-V_i]$, where V_f is the final light intensity translated in voltage, V_i is the initial light intensity, and V_t is the light intensity at the time of measurement. The relative turbidity is an indication of the extent of flocculation. Smaller values correspond to faster flocculation. As the particles flocculate, sedimentation becomes faster and this is the reason that turbidity measurements decrease with time. The data of Table 1 show clearly that seeding increases the magnetic flocculation up to one order of magnitude.

In the remainder of this article, a mathematical analysis is introduced to model particle-particle interactions and magnetic flocculation kinetics of magnetically seeded and non-seeded particle suspensions. This analysis is aiming at providing a basic understanding of particle dynamics in suspensions as well as in HGMF beds. The developed model will be extended in future work to describe experimental data of particle flocculation and filtration and predict the performance of high-gradient magnetic filters.

Table 1. Turbidity Measurements

Time (min)	Relative Turbidity		
	No Field	With Field	With Seeding and Field
0	1	1	1
10	0.95	0.95	0.05
20	0.80	0.60	0
30	0.45	0.20	0
40	0.20	0.10	0
50	0.05	0.05	0
60	0	0	0

THEORETICAL

The forces considered in this work include external forces, such as gravity and magnetism, acting on individual particles and interparticle forces, such as van der Waals, electrostatic, hydrodynamic, and magnetic dipole forces. Brownian relative diffusivity is also considered.

External Forces

External forces due to gravity and magnetism act on particles suspended in a liquid medium. The magnitude of these forces depends on a number of parameters, such as particle size, density, magnetic susceptibility, and magnetic field. The result of these forces is translation of particles in the suspension. Different particles travel at different velocities. The difference of the velocities of two particles is called the relative velocity, V_{12} (m s^{-1}), and is the velocity of one particle with respect to a reference frame based on the center of the other particle (Figure 4).

Gravity: The far-field relative gravitational velocity, $V_{12g}^{(0)}$ (m s^{-1}), for two particles is the difference of their respective individual velocities, $V_{12g}^{(0)} = v_1 - v_2$. Individual particle velocities are obtained from a force balance of gravity,

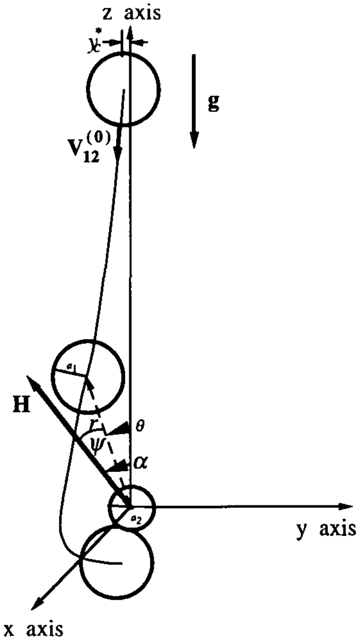

FIGURE 4. Coordinate system for the relative motion of two particles.

buoyancy, and drag forces for each particle. It can be shown that the relative velocity of two particles due to gravity is given by:

$$V_{12g}^{(0)} = \frac{2[(\rho_1 - \rho)a_1^2 - (\rho_2 - \rho)a_2^2]g}{9\eta} \qquad [1]$$

where a_1 and a_2 are the radii (m) of particles 1 and 2 respectively, ρ_1 and ρ_2 are their densities (kg m^{-3}), η is the dynamic viscosity of the surrounding fluid (kg m^{-1} s^{-1}), ρ its density (kg m^{-3}), and g the magnitude of gravitational acceleration (m s^{-2}). The larger particle is designated as subscript 1, and the smaller particle is designated as subscript 2.

Magnetic Attraction: The magnetic force, $\mathbf{F_m}$ (N), on a small particle can be given in terms of the magnetic field (1):

$$\mathbf{F_m} = \frac{2}{3}\pi a^3 \mu_0 \chi \nabla\left(H^2\right) \qquad [2]$$

where χ is the volume magnetic susceptibility (dimensionless), μ_0 is the permeability of free space (μ_0=4 π x10^{-7} V s A^{-1} m^{-1}), and H is the magnitude of the magnetic field vector (A m^{-1}). A force balance of magnetic, buoyancy, and drag forces for each particle gives the relative velocity due to magnetic forces, $\mathbf{V}_{\mathbf{12m}}^{(0)}$ (m s^{-1}), as:

$$\mathbf{V}_{\mathbf{12m}}^{(0)} = \frac{\mu_0 \nabla\left(H^2\right)}{9\eta}\left(\chi_1 a_1^2 - \chi_2 a_2^2\right) \qquad [3]$$

Interparticle Forces

In dilute suspensions, the forces acting between two particles change in strength as one particle approaches the other. The coordinate system used in quantifying the interparticle forces is illustrated in Figure 4. The interparticle forces to be considered in this work are discussed below.

van der Waals Forces: Hamaker (11) calculated the van der Waals interparticle force potential, V_{vdW} (V C), for unequal sized spheres as a function of separation, s (m), and the Hamaker constant, A (J). Later, another expression was derived by Schenkel and Kitchener (12), which incorporates electromagnetic retardation effects in Hamaker's formula.

Electrostatic Forces: Electrostatic repulsion arises when two particles of the same charge sign approach each other and their diffuse layers of ions overlap. There is no general analytical solution providing the electrostatic potential, V_{el} (V C), between spherical particles. For particle size radii much larger than the thickness of the electric double layer and small surface potential, the interaction energy can be calculated from the corresponding flat-plate interactions. Assuming that the interaction energy of two particles is given by the contribution of infinitesimal parallel rings on the surface of the particles, Verwey and Overbeek obtained an approximate analytical expression by integrating the contributions over the entire surface. Improvements to this approximation were made by McCartney and Levine (13), who expressed the potential in terms of a distribution of electric dipoles on the surface of the particles and developed an integral equation, for which a better approximation was derived. Other analytical expressions applicable under various conditions are given in the literature (14,15). Bell et al. (15) derived a formula to be applicable for larger potential values, while Hogg et al. (14) gave an expression for particles of different surface potential useful for heterogeneous particle interactions.

Hydrodynamic Forces: Haber et al. (16) and Zinchenko (17) developed exact solutions for the hydrodynamic resistance to particle collision using the method of bispherical coordinates. Haber et al.'s solution was applied to axisymmetric motion of two drops, and Zinchenko's was applied to the asymmetric motion of drops. Although these solutions were originally calculated for drop motion, they can easily be applied to particle motion by assigning a large value to the ratio of drop viscosity to fluid viscosity (18). Zhang and Davis (18) derived the axisymmetric relative mobility functions $L(s)$ and $G(s)$ from resistance functions obtained by Zinchenko. Similar expressions for the asymmetric relative mobility functions $M(s)$ and $H(s)$ were also found. These hydrodynamic functions were incorporated in this work.

Magnetic Dipole Attraction: The magnetic dipole moment between two particles is expressed with the potential, V_{mag} (V C), given by (19,20):

$$V_{mag} = \frac{4\pi H^2 \mu_0 a_1^3 \chi_1 a_2^3 \chi_2}{9\left(s\frac{a_1+a_2}{2}\right)^3}[(\hat{\mu}_1 \cdot \hat{\mu}_2) - 3(\hat{\mu}_1 \cdot \hat{\mathbf{r}})(\hat{\mu}_2 \cdot \hat{\mathbf{r}})] \qquad [4]$$

where $\hat{\mu}_1$ and $\hat{\mu}_2$ are the unit magnetic dipole vectors of the particles, and $\hat{\mathbf{r}}$ is the unit vector of center-to-center particle separation r (m). The dimensionless particle separation is given by $s = 2r/(a_1 + a_2)$. Since two particles in a uniform magnetic field have the same unit magnetic dipole vector, the first dot product in Eq. [4] becomes 1, and the second and third dot products have the same value. Furthermore, since $\hat{\mu}_1$, $\hat{\mu}_2$, and $\hat{\mathbf{r}}$ are all unit vectors, the value of the second and third dot products is simply the cosine of the angle between $\hat{\mathbf{r}}$ and $\hat{\mu}_i$ for i=1, 2. Eq. [4] can thus be rewritten as

$$V_{mag} = \frac{4\pi H^2 \mu_0 a_1^3 \chi_1 a_2^3 \chi_2}{9\left(s\frac{a_1+a_2}{2}\right)^3}(1 - 3\cos^2 \psi) \qquad [5]$$

where ψ is the angle between the magnetic field and r (see Figure 4). This magnetic dipole interaction depends on the orientation of the particle pair in the magnetic field. An orientation-averaged magnetic dipole interaction has been derived by Chan et al. (21).

The interparticle magnetic potential yields forces along and normal to the line-of-centers:

$$F_r^{magn} = \frac{2\pi H^2 \mu_0 a_1^3 \chi_1 a_2^3 \chi_2}{s^4 \left(\frac{a_1 + a_2}{2} \right)^4} \left\{ \frac{1}{3} + \cos[2(\alpha - \theta)] \right\} \qquad [6]$$

$$F_\theta^{magn} = -\frac{4\pi H^2 \mu_0 a_1^3 \chi_1 a_2^3 \chi_2}{3 s^4 \left(\frac{a_1 + a_2}{4} \right)^4} \sin[2(\alpha - \theta)] \qquad [7]$$

where α is the angle between the direction of the vertical axis and the direction of the magnetic field. The angle ψ defined earlier is related to α by $\psi = |\alpha - \theta|$. It can be shown that the maximum of the tangential force is usually smaller than that of the radial force and both increase as the separation distance decreases. Also the radial force is attractive when $\psi = 0°$, but becomes repulsive when $\psi = 90°$. This observation implies that the direction of the magnetic field will play a significant role on the flocculation frequency.

Equation of Relative Particle Motion

Relative Diffusivity: The relative diffusivity due to Brownian motion for two particles can be expressed as (18):

$$D_{12}^{(0)} = \frac{kT(1 + a_1/a_2)}{6\pi\eta a_1} \qquad [8]$$

where $D_{12}^{(0)}$ is the relative diffusivity between particles 1 and 2 (m^2 s^{-1}), k is the Boltzmann constant (k=1.38x10^{-23} V C K^{-1}), and T is the absolute temperature (K).

Far-Field Relative Velocity: The far-field relative velocity between two particles is the vector addition of the gravitational relative velocity and the magnetic relative velocity in the absence of interparticle forces. Thus, the relative velocity depends on the orientation of the magnetic field, H (A m^{-1}), and the magnetic field gradient (∇H) (A m^{-2}) as compared to the gravitational field. The problem is simplified here by aligning these vectors in the positive or negative vertical direction. This arrangement results in a cylindrical symmetry of forces about the axis along which one particle collides with the other. In the case considered here, the magnetic field and magnetic field gradient vectors are oriented downward, so that the magnetic relative velocity adds to that of gravity. The far-field relative velocity, $V_{12}^{(0)}$, thus becomes:

$$V_{12}^{(0)} = \frac{2[(\rho_1 - \rho)a_1^2 - (\rho_2 - \rho)a_2^2]g + [2H|\nabla H|\mu_0(\chi_1 a_1^2 - \chi_2 a_2^2)]}{9\eta} \quad [9]$$

The relative diffusivity and the far-field relative velocity were related by Davis (22) through two dimensionless parameters, the interparticle force parameter, Q_{12}, and the Péclet number, Pe:

$$Q_{12} \equiv \frac{(a_1 + a_2)V_{12}^{(0)}}{2AD_{12}^{(0)}/kT} \quad [10]$$

$$Pe \equiv \frac{(a_1 + a_2)V_{12}^{(0)}}{2D_{12}^{(0)}} \quad [11]$$

Two limiting cases can be identified: $Pe >> 1$ suggests that the external forces dominate over Brownian diffusion, and $Pe << 1$ means that Brownian diffusion dominates.

Relative Velocity of Approaching Particles: The relative velocity can be found based on a force balance (23,24). In the case of creeping flow, the overall dimensionless relative velocity, $\mathbf{u}_{12}$, is obtained from the relative velocity divided by the far-field relative velocity $V_{12}^{(0)}$:

$$\mathbf{u}_{12} = \left[-L(s)\cos(\theta)\hat{\mathbf{e}}_r + M(s)\sin(\theta)\hat{\mathbf{e}}_\theta\right] - \frac{1}{Q_{12}} G(s) \frac{d(\Phi_{12}/A)}{ds} \hat{\mathbf{e}}_r$$

$$-\frac{D_{12}^{(0)}}{kTV_{12}^{(0)}}\left[G(s)F_r^{mag}\hat{\mathbf{e}}_r - H(s)F_\theta^{mag}\hat{\mathbf{e}}_\theta\right] \qquad [12]$$

$$-\frac{1}{Pe}\left[G(s)\frac{\partial}{\partial s}(\ln p_{12})\hat{\mathbf{e}}_r + \frac{H(s)}{s}\frac{\partial}{\partial \theta}(\ln p_{12})\hat{\mathbf{e}}_\theta\right]$$

where $\hat{\mathbf{e}}_r$ and $\hat{\mathbf{e}}_\theta$ are unit vectors in the radial and tangential direction, respectively, Φ_{12} (V C) is the total interparticle potential given by $V_{vdW} + V_{el}$, and p_{12} represents the normalized probability that particle 1 is at a given position relative to particle 2. Therefore, Eq. [12] includes both deterministic and probabilistic terms, and its solution depends on the functional form of p_{12}. The functions *L(s), M(s), G(s),* and *H(s)* are axisymmetric and asymmetric relative-mobility functions obtained from (17) and (18). A general solution of equation [12], useful for particles in the micron size range, may be obtained using perturbation methods (25). The four terms on the right-hand side of Eq. [12] represent the contributions of (a) external gravity and magnetic forces, (b) interparticle forces including van der Waals and electrostatic, (c) magnetic dipole forces, and (d) Brownian diffusion, respectively.

Flocculation Frequency due to Brownian Diffusion

In the case of $Pe \ll 1$, which usually occurs for submicron particles, Brownian diffusion dominates over external forces. The contribution of external forces is thus negligible, and only interparticle forces and Brownian diffusion are considered. In the absence of the magnetic field, the flocculation frequency has been determined by Zhang and Davis (18) as:

$$F_{12} = \frac{4\pi D_{12}^{(0)}}{\displaystyle\int_{a_1+a_2}^{\infty} \frac{\exp(\Phi_{12}/kT)}{r^2 G(s)} dr} \qquad [13]$$

In the presence of a magnetic field, an integration of the magnetic force is required over all orientations of the particles in the magnetic field. Such an integration has been carried out by Chan et al. (21), and their results have been incorporated in a Brownian diffusion model by Tsouris and Scott (26).

Flocculation Frequency due to Gravity

In the case of $Pe >> 1$, which usually occurs for larger particles, the external forces dominate over Brownian diffusion, and the Brownian diffusion term in Eq. [12] (last term) can be eliminated. Including the magnetic interparticle forces, one can have:

$$\mathbf{u}_{12} = \left[-L(s)\cos(\theta)\hat{\mathbf{e}}_r + M(s)\sin(\theta)\hat{\mathbf{e}}_\theta\right] - \frac{1}{Q_{12}} G(s) \frac{d(\Phi_{12}/A)}{ds} \hat{\mathbf{e}}_r - \frac{D_{12}^{(0)}}{kTV_{12}^{(0)}}\left[G(s)F_r^{mag}\hat{\mathbf{e}}_r - H(s)F_\theta^{mag}\hat{\mathbf{e}}_\theta\right] \qquad [14]$$

By separating Eq. [14] into radial and tangential components and dividing the radial component by the tangential component, the following differential trajectory equation is obtained (27):

$$\frac{ds}{d\theta} = s \frac{-L(s)\cos(\theta) - \frac{G(s)}{Q_{12}^{magn}}\left[\frac{1}{s^4}\left\{\frac{1}{3} + \cos[2(\alpha-\theta)]\right\}\right] - \frac{G(s)}{Q_{12}} \frac{d}{ds}\left(\frac{\Phi_{12}}{A}\right)}{M(s)\sin(\theta) - \frac{H(s)}{Q_{12}^{magn}}\left\{\frac{2}{3s^4}\sin[2(\alpha-\theta)]\right\}} \qquad [15]$$

where Q_{12}^{magn} is defined as:

$$Q_{12}^{magn} \equiv \frac{\left(\frac{a_1 + a_2}{2}\right)^4 V_{12}^{(0)}}{2\pi H^2 \mu_0 \chi_1 \chi_2 a_1^3 a_2^3 D_{12}^{(0)}/kT} \qquad [16]$$

The solution of Eq. [15] gives the trajectory of a particle from an arbitrary starting position relative to a stationary particle. The limiting or critical trajectory for a collision to occur can then be found (see Figure 4). Trajectories which result in flocculation will originate within a certain horizontal distance y_c^* (m) of the z-axis. From this critical radius parameter, the flocculation frequency can be obtained by (18):

$$F_{ij} = V_{ij}^{(0)} \pi y_c^{*2} \qquad [17]$$

In this way, the particle flocculation frequency can be calculated as a function of all parameters of the system. This flocculation frequency can then be used in a bivariate population balance model to estimate the flocculation as a function of time (28):

$$\frac{dn_{ij}}{dt} = \frac{1}{2}\sum_{l=1}^{i-1} \sum_{m=1}^{j} n_{lm} n_{(i-l)(j-m)} F_{lm,(i-l)(j-m)} - \sum_{l=1}^{N_s - i} \sum_{m=1}^{l+N_c^I - 1} n_{ij} n_{lm} F_{ij,lm} \quad [18]$$

where n_{ij} (m^{-3}) is the number of particles of size i and magnetic susceptibility j (class ij), $F_{ij,lm}$ ($m^3\ s^{-1}$) is the flocculation frequency of particles in class ij with particles in class lm, and N_s, N_c^I are the total numbers of size and magnetic susceptibility classes, respectively. Some of the capabilities of this model in describing heterogeneous flocculation between paramagnetic particles of varying magnetic susceptibility are discussed by Tsouris et al. (28).

Finally, the modeling approach described here permits studies of magnetic seeding flocculation in which magnetic particles are added to a suspension of nonmagnetic particles. Initially, flocculation of nonmagnetic with magnetic particles will occur due to both external forces and interparticle forces, but no contribution will be provided by magnetic dipoles. The resulting flocs, however, have higher magnetic susceptibility than the original nonmagnetic particles; therefore in this case, magnetic dipoles will contribute to particle flocculation. This mechanism suggests that magnetic seeding can be mathematically described as a heterogeneous flocculation process, which can be sufficiently handled by the bivariate population balance approach shown by Eq. [18].

RESULTS AND DISCUSSION

An example of particle flocculation under gravity, magnetism, and interparticle forces, based on the model described here, is presented below. The goal of this study is the simulation of magnetic seeding flocculation. The results describe cases where different forces are dominating. Input parameters were chosen to reflect different situations under which flocculation occurs.

Flocculation of Particles Under Gravity, Magnetic, van der Waals, and Hydrodynamic Forces: The first set of the selected input parameters represents the case of the initial stages of magnetic seeding flocculation, when magnetically susceptible particles have just been introduced to the solution. At this point, most flocculation events will be between magnetic and nonmagnetic particles. Figure 5 shows the flocculation frequency for such a case, where a_1=5 μm, a_2=2.5 μm, the magnetically susceptible particle has a susceptibility of χ_1=0.002, and the particles have a density of 3 g/mL. The flocculating particles are assumed to have zero electrostatic potential, and the Hamaker constant is 4.05×10^{-21} J. The flocculation frequency has been estimated by Eq. [17] after solving repeatedly the differential equation shown by Eq. [15]. More details of these calculations are given elsewhere (27). Since in these calculations it is assumed that H and $|\nabla H|$ are constant and have the same direction as gravity, the flocculation frequency is plotted against the magnetic strength, $H|\nabla H|$ (A^2/m^3). It can be observed that whenever there is interaction between magnetic and nonmagnetic particles, the quantities H and $|\nabla H|$ are multiplied by one another wherever they appear in an equation in this study; thus, the two quantities can be grouped as a single variable. Note that this is not true for interactions between two magnetic particles. The results of Figure 5 show that the flocculation frequency increases with increasing magnetic strength. This can be attributed to the fact that the far-field relative velocity increases with the magnetic strength. It can be seen from Eq. [17] that the flocculation frequency is proportional to the relative velocity.

Flocculation of Particles Under Gravity, Magnetic (external), Magnetic Dipole, van der Waals, and Hydrodynamic Forces: This case corresponds to a magnetic particle flocculating with another magnetic particle. The difference with the previous case is that particle flocculation in this situation is influenced by the magnetic dipole force. One particle has a magnetic susceptibility fixed at 0.002, while the other particle has a magnetic susceptibility of 0.001. The gradient of the magnetic induction has been fixed to 100 T/m. All other parameters remain as in the simulation shown in the previous section. The flocculation frequency is shown in Figure 6 as a function of the magnetic induction. As expected, the flocculation frequency increases with increasing magnetic induction.

The results shown in Figures 5 and 6 indicate the capabilities of the model in predicting flocculation frequencies between particles of various properties under the influence of a magnetic field. Although simulation results have not been

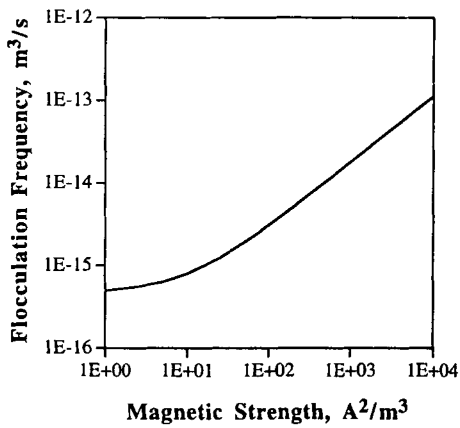

FIGURE 5. Flocculation frequency of two particles under gravity, magnetic, van der Waals, and hydrodynamic forces.

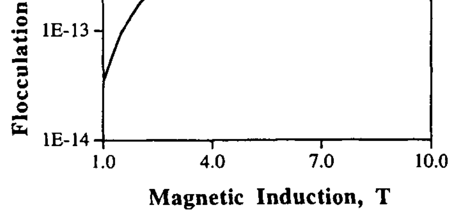

FIGURE 6. Flocculation frequency of two particles under gravity, magnetic, magnetic dipole, van der Waals, and hydrodynamic forces.

compared with experimental data yet, the model developed here provides a basic understanding of fundamental phenomena, such as particle-particle and particle-collector interactions, occurring in HGMF. The developed model will be extended in future work to describe experimental data of particle flocculation and filtration and predict the performance of high-gradient magnetic filters. It is also expected that this model will eventually lead to a tool for design and optimization of magnetic filters for environmental, metallurgical, biochemical, and other applications.

ACKNOWLEDGMENTS

This research was supported by the Division of Chemical Sciences, Office of Basic Energy Sciences, the AR&TD program of Fossil Energy, and the Efficient Separations and Processing Crosscutting Program, Office of Environmental Management, U.S. Department of Energy, under contract DE-AC05-96OR22464 with Lockheed Martin Energy Research Corp. Accordingly, the U.S. Government retains a nonexclusive, royalty-free license to publish or reproduce the published form of this contribution, or allow others to do so, for U.S. Government purposes. During this work, S. Yiacoumi was supported by the School of Civil and Environmental Engineering of Georgia Institute of Technology. The authors are also thankful to Xiaoguang Zhang for providing details of his calculations.

REFERENCES

1. J. Svoboda, *Magnetic Methods for the Treatment of Minerals*, Elsevier, New York, 1987.
2. L. Petrakis, P. F. Ahner, and F. E. Kiviat, Sep. Sci. Technol. 16, 745 (1981).
3. J. Svoboda, M. Lazer, and W. A. M. Te Riele, IEEE Trans. Magn. Mag-23, 283 (1987).
4. J. E. Lawver and D. M. Hopstock, Min. Sci. and Eng. 6, 154 (1974).
5. H. G. Heitmann in *Industrial Applications of Magnetic Separation,* Y. A. Yiu, Ed., Institute of Electrical and Electronics Engineers, Inc., New York, 1979.

6. R. R. Dauer and E. H. Dunlop, Biotech. and Bioeng. 37, 1021 (1991).
7. H. Kolm, J. Kelland, and D. Kelland, Scient. Amer. 46, Nov (1975).
8. C. de Latour, IEEE Trans. Magn. 9, 314 (1973).
9. C. Tsouris, T. C. Scott, and M. T. Harris, Sep. Sci. & Technol. 30 (7-9), 1407 (1995).
10. T. Sugimoto, K. Sakata, and A. Muramatsu, J. Colloid Interface Sci. 159, 372 (1993).
11. H. C. Hamaker, Physica. 4, 1058 (1937).
12. J. H. Schenkel and J. A. Kitchener, Trans. Faraday Soc. 56, 161 (1960).
13. L. N. McCartney and S. Levine, J. Colloid Interface Sci. 30, 345 (1969).
14. R. Hogg, T. W. Healy, and D. W. Fuerstenau, Trans. Faraday Soc. 18, 1638 (1966).
15. G. M. Bell, S. Levine, and L. N. McCartney, J. Colloid Interface Sci. 33, 335 (1970).
16. S. Haber, G. Hetsroni, and A. Solan, Int. J. Multiphase Flow 1, 57 (1973).
17. A. Z. Zinchenko, J. Appl. Math. and Mech. (translation of Prikladnaia Matematika I Mekhanika) 44, 30 (1980).
18. X. Zhang and R. H. Davis, J. Fluid Mech. 230, (1991).
19. S. Chikazumi, *Physics of Magnetism*, John Wiley and Sons, Inc., New York, 1964.
20. R. K. Wangsness, *Electromagnetic Fields*, John Wiley and Sons, Inc., New York, second edition, 1986.
21. D. Y. C. Chan, D. Henderson, J. Barojas, and A. Homola, IBM J. Res. Dev. 29, 11 (1985).
22. R. H. Davis, J. Fluid Mechanics 145, 179 (1984).
23. C. Tien and A. C. Payatakes, AIChE J. 25, 737 (1979).
24. G. K. Batchelor, J. Fluid Mech. 119, 379 (1982).
25. C. Tien, *Granular Filtration of Aerosols and Hydrosols*, Butterworth Publishers, Stoneham, MA, 1989.
26. C. Tsouris and T. C. Scott, J. Colloid Interface Sci. 171, 319 (1995).
27. S. Yiacoumi, D. A. Rountree, and C. Tsouris, J. Colloid Interface Sci., submitted (1996).
28. C. Tsouris, S. Yiacoumi, and T. C. Scott, Chem. Eng. Comm. 137, 147 (1995).